J|A|C|S COMMUNICATIONS

Published on Web 06/30/2010

Holographically Defined Nanoparticle Placement in 3D Colloidal Crystals

Yoonho Jun, Dongguk Yu, Matthew C. George, and Paul V. Braun*

Department of Materials Science and Engineering, Beckman Institute, and Frederick Seitz Materials Research Laboratory, University of Illinois at Urbana−Champaign, Urbana, Illinois 61801

Received March 21, 2010; E-mail: pbraun@illinois.edu

Abstract: We demonstrate an optical interference-based photochemical method for the high-resolution localization of nanoparticles inside colloidal crystals or other porous structures. The method specifically relies on photoinduced inversion of the colloidal crystal surface charge to drive the localized deposition of charged gold nanoparticles. 4-Bromomethyl-3-nitrobenzoic acid (BNBA) was used as a photocleavable linker, and dansylamide was attached to BNBA to increase the absorption at 351 nm. Two-beam interference lithography was used for high-resolution optical patterning of the colloidal crystals; the resulting pattern was then decorated with functional nanoparticles. The periodicity of the pattern was 400 nm, and the width of the gold nanoparticle decorated region was ∼200 nm. Our strategy of using photoswitching in a refractive-index-matched porous medium followed by the attachment of nanoparticles to the photoswitched region should be applicable to wide classes of charged nanoparticles.

Colloidal crystals are formed by the three-dimensional (3D) periodic stacking of typically submicrometer spheres.[1] Other than defects inherent in the assembly process (e.g., surfaces, vacancies, and stacking faults),[2] they possess long-range periodicity with a characteristic lattice constant imposed by the diameter of the colloidal particle. Colloidal crystals are a quite popular starting point for 3D photonic crystals because of their ease of fabrication, optical tunability, and stability. The optical properties of colloidal crystals or inverse opals, which are replicas of colloidal crystals, can be manipulated through materials selection[3−7] or introduction of defined defects.[8−10] However, incorporation of structure on a length scale different than that of the colloidal crystal is possible only through serial optical direct-write strategies,[8,9] and these approaches, which have a minimum feature size defined by the diameter of the focal point, have great difficulty producing structure on length scales well below a micrometer. Tagging of a colloidal crystal over large areas with functional materials (e.g., nanoparticles) in a site-localized fashion on length scales well below a micrometer would provide a number of interesting possibilities, such as all-optical switching,[11] spontaneous emission control of quantum dots,[12] optical metamaterials,[13] and low-threshold lasing.[14] Here we demonstrate an interference lithography approach to high-resolution patterning of colloidal crystals with functional nanoparticles. The method specifically relies on photoinversion of the colloidal crystal surface charge to drive the site-localized deposition of charged gold nanoparticles. The gold dots are subsequently amplified using electroless deposition.

4-Bromomethyl-3-nitrobenzoic acid (BNBA) can directly be used as a photocleavable linker[15,16] to generate localized photoinversion of surface charges inside the colloidal crystal. Photocleavage of this molecule requires a long exposure (∼10 min) at 351 nm, even under high laser powers, because of the very low absorption at this wavelength. Conjugation of dansylamide to the BNBA greatly increases the absorption at 351 nm, reducing the exposure time to ∼60 s. Using this system, as outlined in Figure 1, we can achieve charge inversion upon holographic UV exposure, followed by site-localized deposition of cationic gold nanoparticles and feature amplification by electroless gold deposition. Figure 1b,c shows cross-sectional views of the intensity variation of the two-beam interference patterns applied in this work (see the Supporting Information for experimental details). The final structures after electroless gold deposition are either transmission (Figure 1b) or reflection (Figure 1c) diffraction gratings, depending on the initial laser beam arrangement.

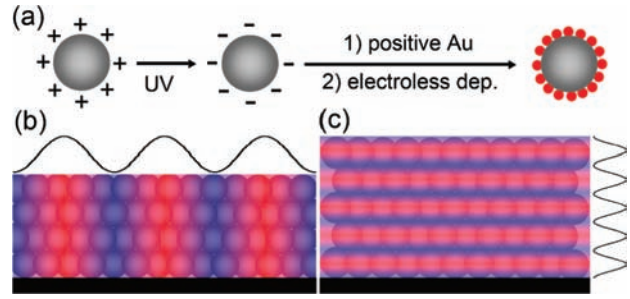

Figure 1. (a) Schematic of UV photoswitching of the colloidal surface charge followed by selective gold decoration and amplification. (b, c) Cross-sectional views of the UV intensity variations for the two-beam interference patterns used in this study (red denotes high intensity and blue low intensity). In (b) the intensity variation is parallel to the substrate, and in (c) it is perpendicular to the substrate.

The silica colloidal crystals were formed on coverslips via convective assembly[1] using 500 nm diameter silica particles. Trimethoxysilylpropylethylenediamine (TMSP-en) was attached on the silica surface. BNBA formed an amide bond with TMSP-en in the presence of 4-(4,6-dimethoxy-1,3,5-triazin-2-yl)-4-methylmorpholinium chloride. Dansylamide was attached, and 4-bromoethane was added to quaternize the dimethylamino end group. After quaternization, the overall surface charge was positive (see the Supporting Information). The functionalized colloidal crystal was filled with dimethylformamide (DMF, used as an index-matching fluid) to reduce scatter during two-beam interference pattern generation. Upon UV exposure, bond cleavage occurred, exposing neutral aldehyde groups (Figure 2c). Because the native surface charge of the silica is negative, the overall surface charge switches from positive to negative upon loss of the positive quaternary ammonium groups.

To confirm photocleavage, a transmission grating sample was labeled with fluorescein-5-thiosemicarbazide (5-FTSC), which reacts with aldehyde groups formed by the UV exposure, and imaged via confocal microscopy (Figure 2). Under the 488 nm excitation used for the confocal microscopy, emission was observed only from the 5-FTSC-labeled regions, as dansylamide has negligible absorption at 488 nm. Confocal microscopy images of plane and cross-sectional views of a sample exposed using the two-beam interference pattern intensity profile of Figure 1b are shown in Figure 2a,b, respectively. The left and right panels of Figure 2c show the structure of the molecules in the unexposed and exposed regions, respectively after 5-FTSC labeling. The periodic pattern of bright and dark planes perpendicular to the substrate matches the interferogram. The fluorescence is greatest in the center of each plane, and falls off to either

10.1021/ja1023628

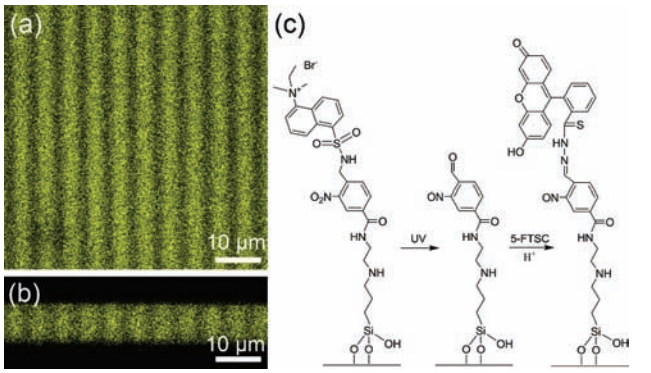

Figure 2. (a) Plain and (b) cross-sectional laser scanning confocal microscope images (488 nm excitation, 500−540 nm detection) of a sample exposed using the intensity profile shown in Figure 1b after 5-FTSC labeling. (c) Chemical schematics of the surface chemistry (left) before UV exposure, (middle) after UV exposure, and (right) after 5-FTSC labeling. Bright areas in (a) and (b) correspond to the high-intensity region where photocleavage and subsequent 5-FTSC labeling occurred, and dark areas represent the low-intensity regions still functionalized with the original dansylamide. As can be observed in the cross-sectional image (b), the pattern was formed through the ~10 μm sample thickness.

side, indicating the expected relationship between the exposure dose and photocleavage. The periodicity of this pattern is about 6 μm, and the pattern was formed through the sample thickness.

The charge inversion upon UV exposure enabled the high-resolution localized deposition of positively charged gold nanoparticles. Interferometrically exposed samples were first immersed in the solution containing the positively charged gold nanoparticles for 24 h and then, to amplify the gold nanoparticles, a gold electroless plating solution for 1−2 days. Figure 3a presents (top) schematic and (bottom) scanning electron microscopy (SEM) cross-sectional images of the gold-nanoparticle-decorated and amplified sample exposed as illustrated in Figure 1b. The gold nanoparticle distribution and density closely matches the light intensity distribution, as shown in the high-resolution images in Figure 3b, which were taken from the areas noted in Figure 3a. The long-range periodicity of this transmission diffraction grating was demonstrated via optical diffraction at 532 nm (Figure 3c). DMF was used as an index-matching fluid, so the diffraction spots were exclusively a result of the periodic metal nanoparticle distribution. With a reflection grating geometry (Figure 1c), high-resolution patterning could be demonstrated. Here the periodicity was 400 nm, and the width of the gold-nanoparticle-decorated region was only ~200 nm (Figure 3d,e). These samples were also decorated with gold nanoparticles following the same procedure as for Figure 3a. The red dots have been added to the image to make the gold nanoparticles more distinct. The original image is shown in the Supporting Information, where a sample with a higher gold nanoparticle coverage is also presented.

In conclusion, we have demonstrated a versatile and unique method for the high-resolution localization of nanoparticles inside colloidal crystals or other porous structures. This method provides much higher coverage of gold nanoparticles than direct-assembly approaches such as volume holography,[17] in which the interaction of the nanoparticle with the patterning light source needs to be considered. Here the nanoparticles are introduced after the patterning step, so the optical activity of the nanoparticles does not have to be considered. Our strategy of using photoswitching in a refractive-index-matched porous medium followed by the chemical attachment of nanoparticles to the photoswitched region is general and should be applicable to wide classes of nanoparticles.

Acknowledgment. This work was primarily supported by the DOE "Light−Material Interactions in Energy Conversion" Energy Frontier Research Center under Grant DE-SC0001293. We thank Abigail Juhl and Sidhartha Gupta of the authors' laboratory for experimental assistance.

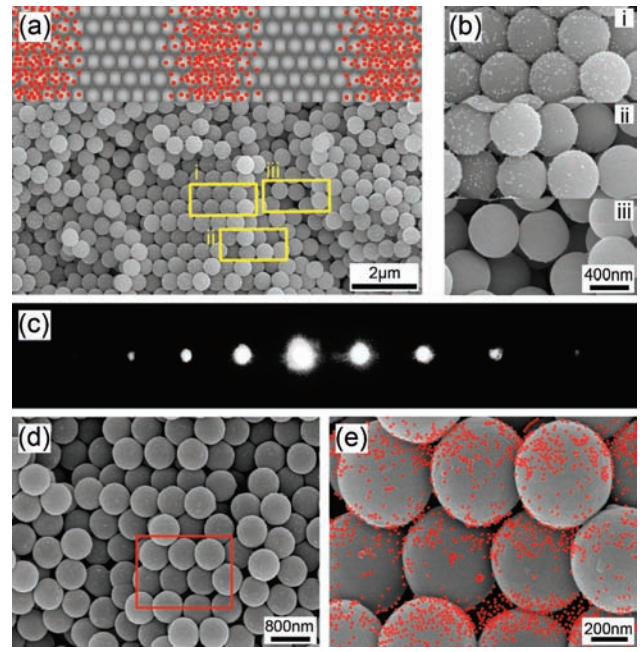

Figure 3. (a) (top) Schematic of the expected gold nanoparticle distribution and (bottom) low-magnification SEM micrograph of a cross section of a gold-nanoparticle-labeled colloidal crystal at the same scale as the top. The areas noted with the yellow boxes are presented in (b). In (b), gold nanoparticles are present across box (i), present only in the left portion of box (ii), and absent from the region shown in box (iii), closely matching the expected nanoparticle distribution. (c) Transmission diffraction grating of a refractive-index-matched nanoparticle-loaded colloidal crystal upon illumination with 633 nm laser radiation, demonstrating the periodic nanoparticle arrangement. (d) Low-magnification SEM micrograph of a gold-nanoparticle-loaded reflection diffraction grating. The boxed region is shown at higher magnification in (e). In (e), the gold nanoparticles have been colored red for ease of identification.

Supporting Information Available: Experimental procedures and unenhanced SEM images. This material is available free of charge via the Internet at http://pubs.acs.org.

References

(1) Jiang, P.; Bertone, J. F.; Hwang, K. S.; Colvin, V. L. *Chem. Mater.* **1999**, *11*, 2132–2140.
(2) Wei, H.; Meng, L.; Jun, Y.; Norris, D. J. *Appl. Phys. Lett.* **2006**, *89*, 241913.
(3) Braun, P. V.; Wiltzius, P. *Nature* **1999**, *402*, 603–604.
(4) Norris, D. J.; Vlasov, Y. A. *Adv. Mater.* **2001**, *13*, 371–376.
(5) Puzzo, D. P.; Arsenault, A. C.; Manners, I.; Ozin, G. A. *Angew. Chem., Int. Ed.* **2009**, *48*, 943–947.
(6) Vlasov, Y. A.; Bo, X. Z.; Sturm, J. C.; Norris, D. J. *Nature* **2001**, *414*, 289–293.
(7) Blanco, A.; Chomski, E.; Grabtchak, S.; Ibisate, M.; John, S.; Leonard, S. W.; Lopez, C.; Meseguer, F.; Miguez, H.; Mondia, J. P.; Ozin, G. A.; Toader, O.; van Driel, H. M. *Nature* **2000**, *405*, 437–440.
(8) Rinne, S. A.; Garcia-Santamaria, F.; Braun, P. V. *Nat. Photonics* **2008**, *2*, 52–56.
(9) Jun, Y.; Leatherdale, C. A.; Norris, D. J. *Adv. Mater.* **2005**, *17*, 1908–1911.
(10) Palacios-Lidon, E.; Galisteo-Lopez, J. F.; Juarez, B. H.; Lopez, C. *Adv. Mater.* **2004**, *16*, 341–345.
(11) Nakamura, H.; Sugimoto, Y.; Kanamoto, K.; Ikeda, N.; Tanaka, Y.; Nakamura, Y.; Ohkouchi, S.; Watanabe, Y.; Inoue, K.; Ishikawa, H.; Asakawa, K. *Opt. Express* **2004**, *12*, 6606–6614.
(12) Lodahl, P.; van Driel, A. F.; Nikolaev, I. S.; Irman, A.; Overgaag, K.; Vanmaekelbergh, D. L.; Vos, W. L. *Nature* **2004**, *430*, 654–657.
(13) Gwinner, M. C.; Koroknay, E.; Fu, L. W.; Patoka, P.; Kandulski, W.; Giersig, M.; Giessen, H. *Small* **2009**, *5*, 400–406.
(14) Scotognella, F.; Puzzo, D. P.; Monguzzi, A.; Wiersma, D. S.; Maschke, D.; Tubino, R.; Ozin, G. A. *Small* **2009**, *5*, 2048–2052.
(15) Plunkett, K. N.; Mohraz, A.; Haasch, R. T.; Lewis, J. A.; Moore, J. S. *J. Am. Chem. Soc.* **2005**, *127*, 14574–14575.
(16) Wu, C. L.; Chen, C.; Lai, J. P.; Chen, J. B.; Mu, X.; Zheng, J. S.; Zhao, Y. B. *Chem. Commun.* **2008**, 2662–2664.
(17) Goldenberg, L. M.; Sakhno, O. V.; Smimova, T. N.; Helliwell, P.; Chechik, V.; Stumpe, J. *Chem. Mater.* **2008**, *20*, 4619–4627.

JA1023628